The causal effect of epigenetic aging on intracerebral hemorrhage is not mediated by frontal network function: A Mendelian randomization study

Keywords
genome-wide association studies, intracerebral hemorrhage, Mendelian randomization, epigenetic clocks, aging markers

Abstract

Introduction
The association between epigenetic clocks and intracerebral hemorrhage (ICH) remains poorly understood. This study investigated whether specific brain imaging phenotypes play a mediating role in the causal pathway from epigenetic aging to ICH.

Material and methods
We utilized genome-wide association study (GWAS) summary statistics for four epigenetic clocks and two related biomarkers (from a large-scale meta-analysis), 20 brain functional imaging phenotypes, and ICH (FinnGen R12). A two-sample Mendelian randomization (MR) analysis was performed to estimate the total causal effect, followed by a two-step mediation analysis to explore potential neural mediators. The inverse variance weighted (IVW) method was employed as the primary analysis. Comprehensive sensitivity analyses, including MR-Egger, weighted median, and RadialMR, were conducted to ensure result robustness and correct for horizontal pleiotropy.

Results
Genetically predicted accelerated PhenoAge was causally associated with an increased risk of ICH (OR = 1.08, 95% CI: 1.03–1.13). While an exploratory association was identified between PhenoAge and a frontal network phenotype (pheno16) after outlier removal, pheno16 showed no causal effect on ICH. Consequently, the hypothesized mediating pathway (PhenoAge → frontal network function → ICH) was not supported. Furthermore, a supplementary analysis revealed no causal link between PhenoAge and white matter hyperintensities, a marker of cerebral small vessel disease.

Conclusions
The study provides genetic evidence that the acceleration of the epigenetic clock PhenoAge may be causally associated with ICH. However, the hypothesized mediating pathway via changes in frontal network function (pheno16) was not supported, suggesting that other biological mechanisms may be involved.

The causal effect of epigenetic aging on intracerebral hemorrhage is not mediated by frontal network function: A Mendelian randomization study

Running Title: MR: epigenetic aging and intracerebral hemorrhage

Yunyao Li[1], Xinyu Cheng[2], Qiang Wang[2], Jianwei Guan[2*]

[1]Department of Hematology/Oncology, Children's Medical Center, Sun Yat-sen Memorial Hospital, Sun Yat-sen University, Guangzhou 510120, China

[2]Department of Neurosurgery, Zhujiang Hospital, Southern Medical University, The National Key Clinical Specialty, The Engineering Technology Research Center of Education Ministry of China, Guangdong Provincial Key Laboratory on Brain Function Repair and Regeneration, The Neurosurgery Institute of Guangdong Province, Guangzhou 510282, China

[*]Corresponding author

Jianwei Guan

E-mail: guanchuhu@163.com

Tel: +8618620570726

ABSTRACT

Introduction: The association between epigenetic clocks and intracerebral hemorrhage (ICH) remains poorly understood. This study investigated whether specific brain imaging phenotypes play a mediating role in the causal pathway from epigenetic aging to ICH.

Methods: We utilized genome-wide association study (GWAS) summary statistics for four epigenetic clocks and two related biomarkers (from a large-scale meta-analysis), 20 brain functional imaging phenotypes, and ICH (FinnGen R12). A two-sample Mendelian randomization (MR) analysis was performed to estimate the total causal effect, followed by a two-step mediation analysis to explore potential neural mediators. The inverse variance weighted (IVW) method was employed as the primary analysis. Comprehensive sensitivity analyses, including MR-Egger, weighted median, and RadialMR, were conducted to ensure result robustness and correct for horizontal pleiotropy.

Results: Genetically predicted accelerated PhenoAge was causally associated with an increased risk of ICH (OR = 1.08, 95% CI: 1.03–1.13). While an exploratory association was identified between PhenoAge and a frontal network phenotype (pheno16) after outlier removal, pheno16 showed no causal effect on ICH. Consequently, the hypothesized mediating pathway (PhenoAge → frontal network function → ICH) was not supported. Furthermore, a supplementary analysis revealed no causal link between PhenoAge and white matter hyperintensities, a marker of cerebral small vessel disease.

Conclusion: The study provides genetic evidence that the acceleration of the epigenetic clock PhenoAge may be causally associated with ICH. However, the

hypothesized mediating pathway via changes in frontal network function (pheno16) was not supported, suggesting that other biological mechanisms may be involved.

Keywords: Mendelian randomization, intracerebral hemorrhage, epigenetic clocks, aging markers, genome-wide association studies.

Introduction

Intracerebral hemorrhage (ICH), a devastating subtype of stroke, accounts for 10-20% of all strokes and is associated with extremely high rates of mortality and morbidity [1, 2]. Although hypertension and advanced age are well-established major risk factors, a substantial portion of ICH risk cannot be fully explained by traditional factors, suggesting the existence of other, under-recognized pathophysiological mechanisms [1, 3]. Therefore, identifying novel causal risk factors is crucial for the prevention and risk stratification of ICH.

In recent years, the discrepancy between biological age and chronological age has been recognized as a more precise indicator of an individual's health status and disease susceptibility [4]. Epigenetic clocks, particularly age estimators based on DNA methylation (DNAm), have emerged as powerful tools for quantifying the biological aging process [4]. First-generation epigenetic clocks, such as HorvathAge and HannumAge, primarily reflect intrinsic cellular aging processes [5-7]. In contrast, second-generation clocks like GrimAge and PhenoAge, which integrate blood biochemical markers associated with morbidity and mortality risk (such as smoking-related DNAm sites or C-reactive protein), have been shown to more accurately predict the risk of various age-related diseases, including cardiovascular disease and all-cause mortality [5, 8, 9].

Observational studies have provided preliminary evidence of a potential association between epigenetic age acceleration and stroke risk [10, 11]. However, these studies are susceptible to confounding factors (e.g., lifestyle, socioeconomic status) and reverse causation, preventing the establishment of a causal link [4, 10]. Furthermore, the precise mechanism through which epigenetic aging increases ICH risk remains an unresolved scientific question [10, 12]. A plausible hypothesis is that systemic

biological aging processes may mediate their pathogenic effects by compromising the structural and functional integrity of the brain itself [12, 13]. Emerging evidence indicates that systemic inflammation and endothelial dysfunction associated with aging and vascular risk factors preferentially affect highly connected, energy-demanding brain hubs, such as the default mode network (DMN) and the central executive network (CEN) [14-16]. Early alterations in the function of these networks, which can be quantified using resting-state functional magnetic resonance imaging (fMRI), may occur before overt structural damage and serve as sensitive indicators of brain physiological vulnerability [17-19]. Therefore, it can be hypothesized that epigenetic aging may increase the risk of ICH under stressors like blood pressure fluctuations by disrupting the functional stability of these critical cognitive networks, thereby serving as an intermediate link connecting epigenetic aging and ICH [12, 20, 21].

The Mendelian randomization (MR) method, which utilizes genetic variants as instrumental variables, can effectively emulate a randomized controlled trial, thereby minimizing the confounding and reverse causation biases prevalent in traditional observational studies [22-24]. Accordingly, this study leverages a two-sample MR framework to systematically investigate the causal pathway from epigenetic aging to ICH. Our primary objective was to determine the causal effect of accelerated epigenetic aging on ICH risk. Subsequently, we performed a mediation analysis to formally test whether this effect is mediated by specific alterations in frontal lobe network function. This research aims to provide novel genetic evidence for the etiology of ICH and to clarify the role of neuroimaging phenotypes in its pathogenesis.

Materials and Methods

Study design

In this study, single-nucleotide polymorphisms (SNPs) identified from GWAS served as genetic instrumental variables (IVs). As presented in **Figure 1**, our bidirectional two-sample MR analysis was founded on three assumptions [25]: 1) Relevance assumption: The IVs were significantly associated with the exposure. 2) Independence assumption: The IVs were uncorrelated with variables influencing both exposure and outcome. 3) Exclusion assumption: The IVs influenced the outcome exclusively through their impact on the exposure. Modern MR approaches, which accommodate correlated pleiotropy, have examined bidirectional causation. Ethical approval for this study was not required, given that the GWAS data had already been ethically approved. Our study adheres to the STROBE-MR guidelines for enhancing the reporting of observational studies that utilize MRI.

A three-step MR framework was employed [26]. Step 1: A standard MR analysis to test the causal relationship between each epigenetic marker (exposure) and ICH (outcome). Step 2: For any epigenetic marker found to have a causal effect on ICH in Step 1, its causal effect on each of the 20 brain imaging phenotypes (as outcomes) was evaluated. Step 3: For any brain imaging phenotype found to be causally influenced by the epigenetic marker in Step 2, its causal effect (as an exposure) on ICH (as the outcome) was assessed to test the full mediation pathway. In addition to the three-step mediation analysis, an exploratory MR analysis was conducted to test the direct causal effect of PhenoAge on a key structural brain phenotype (WMH).

Data sources

GWAS summary statistics for ICH were obtained from the FinnGen consortium (Release 12). Trait: Intracerebral hemorrhage. GWAS ID: I9_ICH. Sample size: 5112

cases and 450,016 controls. Number of SNPs: Not specified in source, obtained from full summary data. The brain imaging data were obtained from the GWAS summary statistics for 20 brain imaging phenotypes (node-based functional connectivity) in a publicly available dataset (https://zenodo.org/records/5775047). The 20 brain imaging phenotypes are node-based functional connectivity metrics derived from resting-state fMRI, with detailed anatomical locations and network affiliations as described by the original GWAS study (e.g., pheno16 is a node in the frontal lobe belonging to the Salience and Central Executive networks) (Supplementary Table S1).

Following a previous MR study [27], four epigenetic clocks (PhenoAge, GrimAge, HannumAge, and HorvathAge) and two related biomarkers (granulocyte proportions and plasminogen activator inhibitor-1 [PAI-1]) were selected as exposures. To avoid population stratification bias, GWAS data from European ancestry populations were used, obtained from a large-scale meta-analysis [28] via https://datashare.ed.ac.uk/handle/10283/3645. Specific sample sizes were confirmed from recent publications [29, 30].

GWAS summary statistics for WMH were obtained from https://hugeamp.org/phenotype.html?phenotype=WMH, covering 34,467 individuals.

Instrumental variable selection

For exposures in steps 1 and 2, SNPs were selected at the genome-wide significance threshold of $P < 5 \times 10^{-8}$ [31]. However, for granulocyte proportions and GrimAge, this strict threshold yielded an insufficient number of IVs. Therefore, to ensure a sufficient number of instruments for a robust MR analysis, a more permissive threshold ($P < 5 \times 10^{-6}$) was employed for these two exposures. For step 3, SNPs associated with the brain imaging phenotypes were selected at $P < 5 \times 10^{-8}$ (with the exception of pheno19, which used $P < 5 \times 10^{-6}$) [31]. To ensure instrument validity,

several quality control steps were applied. SNPs with a minor allele frequency (MAF) > 0.01 were included, and those in linkage disequilibrium (LD) were pruned based on $R^2 < 0.001$ within a 10,000 kb window [32]. If an IV was unavailable in the outcome GWAS, a proxy SNP with high LD ($R^2 > 0.8$) was substituted. Finally, the F-statistic for each IV was calculated as $F = R^2 \times (N-2) / (1-R^2)$, where R^2 is the proportion of variance in the exposure explained by the SNP. Only IVs with $F > 10$ were retained to mitigate weak instrument bias [33], especially for exposures for which a relaxed selection threshold had to be used (i.e., granulocyte proportions and GrimAge). To mitigate the risk of weak instrument bias potentially arising from this relaxed threshold, we ensured that the F-statistic for every selected IV was substantially greater than the conventional threshold of 10.

MR analysis

The primary method employed in this analysis was the inverse variance weighted (IVW) approach, which estimates the causal association between exposure and outcome by calculating the odds ratio (OR) and its 95% confidence interval (CI). The IVW method [34], pivotal for interpreting MR results, computes a weighted average of effect sizes, with weights assigned as the inverse of the variance of each SNP. To ensure the robustness of our findings, we complemented the IVW method with additional analyses, including MR-Egger, weighted median, and weighted mode methods. The MR-Egger approach accounts for the potential presence of a horizontal pleiotropy intercept, providing an accurate estimation of the causal association even in the presence of pleiotropy bias [35]. The weighted median method assumes that half of the instrumental variables are valid, thereby examining the causal association between exposure and outcome [36]. All analyses were conducted using the "TwoSampleMR" package in R version 4.0.5, with visualization facilitated through

scatter plots and sensitivity analysis plots. The Benjamini-Hochberg method was used to apply a false discovery rate (FDR) correction for multiple testing, with $P_{FDR} < 0.05$ considered statistically significant [37].

Sensitivity analysis

Sensitivity analysis was conducted to detect potential pleiotropy in the MR study. Cochran's Q test was used to assess heterogeneity among the IVs [38], with a P-value greater than 0.05 indicating low heterogeneity, suggesting that the valuations among IVs vary randomly and have minimal impact on the IVW results. Considering the influence of genetic pleiotropy on the estimation of the association effect, the MR-Egger regression method was employed to explore the presence of horizontal pleiotropy. A non-significant intercept in the MR-Egger regression indicates the absence of pleiotropy. Additionally, the MR pleiotropy residual sum and outlier (MR-PRESSO) method was utilized to identify and exclude potential outliers (SNPs with $P < 0.05$) [39], followed by re-estimation of the causal association to correct for horizontal pleiotropy. Leave-one-out analysis was performed to test the robustness and consistency of the results, ensuring that no single SNP disproportionately influenced the overall findings [40]. For analyses showing significant heterogeneity, a radial MR analysis was performed to identify and manually remove outlier IVs. The MR analysis was then repeated [41].

Results

Causal Association Between Epigenetic Clocks and ICH

Instrumental Variable Selection for Epigenetic Clocks

Granulocyte proportions: 19 IVs were selected. The mean F-statistic was 26.51 (range: 19.84-75.93). GrimAge: 27 IVs were selected. The mean F-statistic was 25.19 (range:

21.10-45.49). HannumAge: 9 IVs were selected. The mean F-statistic was 48.31 (range: 30.82-98.89). HorvathAge: 24 IVs were selected. The mean F-statistic was 55.47 (range: 31.08-239.73). PAI-1: 5 IVs were selected. The mean F-statistic was 85.83 (range: 49.50-162.55). PhenoAge: 11 IVs were selected. The mean F-statistic was 51.16 (range: 31.77-89.39). For the analysis with ICH as the outcome, one SNP was not found in the summary data, and no suitable proxy was available. One palindromic SNP was removed during data harmonization.

PhenoAge Shows a Robust Causal Association with Increased ICH Risk

Genetically predicted acceleration of PhenoAge was causally associated with an increased risk of ICH (IVW OR = 1.08, 95% CI: 1.03–1.13, $P = 6.0 \times 10^{-4}$; PFDR = 0.0035). No other epigenetic clock or biomarker showed a statistically significant causal association with ICH risk (Table 1 and Figure 2). For the association between PhenoAge and ICH, the MR-Egger intercept test did not indicate directional pleiotropy (P = 0.11).

Cochran's Q test showed no evidence of heterogeneity (P = 0.73). The MR-PRESSO global test did not detect any significant outliers (P = 0.76). Detailed results are provided in Supplementary Tables S2 and S3.

Causal Association Between PhenoAge and Brain Imaging Phenotypes

Instrumental Variables for PhenoAge

As PhenoAge was the only significant exposure from Step 1, it was carried forward as the exposure for Step 2. All 11 IVs for PhenoAge were available in the brain imaging GWAS datasets, and no SNPs were removed during harmonization.

Exploratory analysis suggests a potential association between PhenoAge and pheno16 after outlier removal

In the primary Mendelian randomization analysis, genetically predicted PhenoAge

acceleration was not causally associated with any of the 20 tested brain imaging phenotypes after applying FDR correction for multiple testing (all PFDR > 0.05, Table 2).

However, we observed significant heterogeneity in the analyses for several phenotypes, including pheno1, pheno3, pheno5, pheno13, pheno14, and pheno16 (Cochran's Q P < 0.05, Supplementary Table S4-S5), suggesting the potential influence of outlier instrumental variables. To investigate this, we conducted an exploratory sensitivity analysis using the RadialMR method to identify and remove these outliers. After outlier removal, heterogeneity was resolved for all aforementioned associations (all P > 0.05, Supplementary Table S6).

Notably, for the pheno16 outcome (a functional connectivity node located in the frontal lobe and integral to both the salience and central executive networks), after removing three influential IVs (rs11253338, rs1990053, rs6531114), a nominally significant association with PhenoAge emerged (IVW OR = 1.02, 95% CI: 1.003–1.04, P = 0.0227). However, this finding should be interpreted with considerable caution, as it was not present in the primary analysis and became apparent only after a data-driven correction. The subsequent sensitivity analyses for this corrected PhenoAge-pheno16 association showed no evidence of directional pleiotropy (MR-Egger intercept P = 0.182) or remaining outliers (MR-PRESSO global test P > 0.05) (Supplementary Tables S7-S8).

Causal Association Between Brain Imaging Phenotype pheno16 and ICH

Instrumental Variable Selection for brain imaging

As pheno16 was the only significant outcome from Step 2, it was carried forward as the exposure for Step 3. Seventeen IVs were selected for pheno16. The mean F-statistic was 70.75 (range: 31.35–215.2), and the R^2 was 0.0361. All IVs were

available in the ICH GWAS, with two SNPs (rs225644 and rs12424773) being replaced by proxies (rs225647 and rs4842318, respectively). No SNPs were removed during harmonization.

Brain Imaging Phenotype pheno16 Is Not Causally Associated with ICH

There was no statistically significant causal association between a genetic predisposition to altered pheno16 and the risk of ICH (IVW OR = 0.91, 95% CI: 0.71–1.17, P = 0.475) (Table 3).

The initial analysis showed evidence of both heterogeneity (Cochran's Q P = 0.0011) and directional pleiotropy (MR-Egger intercept P = 0.041). MR-PRESSO also identified one outlier (rs429358). After removing three outliers identified by RadialMR (rs225644, rs429358, rs9426785), both heterogeneity (P = 0.529) and pleiotropy (MR-Egger intercept P = 0.072) were no longer significant. The null causal estimate remained unchanged (IVW OR after correction = 0.93, 95% CI: 0.78–1.10, P = 0.369) (Supplementary Tables S9-S13).

Exploratory Analysis of the Causal Effect of PhenoAge on White Matter Hyperintensities

A supplementary analysis was performed to examine a possible causal association between PhenoAge and WMH. The IVW showed no causal association between PhenoAge and WMH (OR = 1.0171, 95%CI: 0.9838-1.0516, P = 0.3181) (Supplementary Table S14). No heterogeneity (P = 0.1112), horizontal pleiotropy (P = 0.4930), or outliers (P = 0.1297) were observed (Supplementary Table S15-S16). The results showed no evidence of a causal association between genetically predicted PhenoAge and WMH.

Discussion

In this study, a systematic three-step MR framework was employed to investigate the causal relationship between epigenetic aging and ICH, as well as its potential neuroimaging-mediated mechanisms. The study yielded several key findings. First, among multiple epigenetic markers, only the genetically predicted acceleration of PhenoAge demonstrated a robust causal association with an increased risk of ICH. Second, after a rigorous sensitivity analysis corrected for the distorting effects of outlier SNPs, we uncovered a possible causal association between accelerated PhenoAge and pheno16, a functional connectivity node located in the frontal lobe and integral to both the salience and central executive networks. Third, and importantly, we found no causal effect of PhenoAge on WMH, a major structural brain phenotype. Finally, this brain imaging phenotype itself had no causal effect on ICH risk. This indicates that while PhenoAge impacts both brain network function and ICH risk, the specific tested pathway is not the primary mechanism, suggesting other factors mediate the association.

The core finding of this study was that genetically predicted PhenoAge acceleration was causally associated with ICH (OR = 1.08). This result was consistent across multiple MR methods and withstood sensitivity analyses, with no evidence of interference from horizontal pleiotropy or heterogeneity, thus supporting its reliability. Notably, other epigenetic clocks, including HorvathAge, HannumAge, and GrimAge, as well as aging-related biomarkers like PAI-1 and granulocyte proportions, did not show causal associations with ICH. The specificity of this finding has important biological implications [42-44]. Unlike first-generation clocks, PhenoAge was developed by incorporating various clinical biochemical indicators that reflect physiological function, such as albumin, creatinine, C-reactive protein (CRP), and lymphocyte percentage [45]. Consequently, PhenoAge is not merely a marker of

intrinsic cellular aging but a comprehensive indicator of systemic physiological dysregulation, chronic inflammation, and metabolic stress [43, 45]. The pathology of ICH, particularly hypertension-related deep ICH, is rooted in lipohyalinosis of deep penetrating arteries, a process closely related to chronic inflammation, endothelial dysfunction, and vascular wall remodeling [46-48]. Our findings strongly suggest that it is this state of systemic physiological decline captured by PhenoAge, rather than cellular aging alone, that constitutes an upstream causal driver of ICH [48], offering a new perspective that ICH may be a manifestation of accelerated systemic biological aging within the cerebrovascular system [47, 48].

To elucidate the biological mechanism linking PhenoAge to ICH, we investigated the potential mediating role of brain imaging phenotypes [49, 50]. In our exploratory analysis, after excluding several outlier SNPs with potential horizontal pleiotropy, we identified a nominally significant causal association between accelerated PhenoAge and the frontal functional phenotype (pheno16). This observation should be viewed as an exploratory signal rather than a definitive finding, as it did not reach significance in the primary analysis and depends on a data-driven adjustment that may increase the risk of false positives. Moreover, although we conducted extensive sensitivity analyses, residual horizontal pleiotropy cannot be fully excluded, particularly for associations that depend on post hoc outlier exclusion. Although the removal of outliers is a standard procedure in MR studies to assess heterogeneity, it cannot substitute for the robustness of the primary analysis. Consequently, this potential association requires rigorous replication and validation in larger, independent cohorts to confirm its reliability. Nevertheless, it has been reported that accelerated biological aging, as captured by PhenoAge, does exert a causal influence on the functional integrity of higher-order cognitive networks involving the frontal lobe [51, 52]. This

is a biologically plausible finding, as these networks are known to be vulnerable to vascular risk factors and aging. Rather than being a weak or uncertain signal, this result highlights the importance of robust sensitivity analyses in MR studies to identify true biological effects that might otherwise be obscured by complex genetic architectures. The observed potential association between PhenoAge and pheno16 is compelling because it implicates two higher-order cognitive networks, the Salience Network and the Central Executive Network, which play essential roles in attention, executive function, and decision-making. Both networks are especially vulnerable to age-related and vascular changes, contributing to cognitive impairment in aging populations. Thus, these findings support the hypothesis that epigenetic aging may adversely impact brain health by disrupting key frontal-lobe hubs responsible for cognitive control and adaptive behaviors [53-55].

More critically, despite establishing a potential link between PhenoAge and pheno16, our study found no evidence that this brain phenotype itself increases the risk of ICH. This decisive null result breaks the hypothesized mediation chain and suggests a crucial pathophysiological distinction: the systemic effects of biological aging on brain network function may represent an earlier and separate process from the specific vascular pathologies that lead to hemorrhage. There are several possible explanations for this finding. Our findings, which do not support a mediating role of frontal network function, lead us to hypothesize that the pathogenic effect of PhenoAge on ICH may be transmitted predominantly through more direct vascular and molecular mechanisms. However, this interpretation remains speculative and requires empirical validation. Specifically, emerging evidence suggests that epigenetic aging influences vascular health via pathways such as enhanced inflammation, oxidative stress, and endothelial dysfunction, rather than through alterations in large-scale brain networks.

Future MR studies incorporating genetic instruments for endothelial function, inflammation, or blood–brain barrier integrity are needed to directly test these hypotheses and clarify the mechanistic pathways linking epigenetic aging to ICH. The systemic inflammation and metabolic stress captured by PhenoAge can induce endothelial dysfunction and compromise blood-brain barrier integrity. These early microvascular changes can disrupt neurovascular coupling and the delicate energy metabolism of high-demand brain hubs, manifesting as altered functional connectivity long before structural failure. This aligns with the idea that the effect is primarily vascular rather than a consequence of altering macroscopic brain functional network structures [42, 56]. Second, ICH is fundamentally a structural event—the physical rupture of a vessel. As a macroscopic imaging indicator of network synchrony, pheno16 inherently lacks the sensitivity and specificity to capture the microscopic structural changes, such as lipohyalinosis or arteriolosclerosis, that are directly related to vascular rupture [57, 58]. Third, the possibility that other brain regions or networks not tested in our study act as mediators cannot be excluded [59, 60]. Therefore, our results suggest that future research into the pathogenic mechanisms of PhenoAge should shift its focus from macro-level brain structures to the vascular biology and molecular pathways that precipitate cerebrovascular rupture. To evaluate these hypotheses, future research could construct Mendelian randomization models using genetic instruments specifically associated with endothelial function, blood-brain barrier integrity, or defined inflammatory pathways. In addition, leveraging functional genomics data to annotate PhenoAge-linked SNPs may help elucidate their molecular roles within vascular cells and underlying biological mechanisms.

To elucidate the pathways connecting PhenoAge with intracerebral hemorrhage (ICH), the mediation analysis systematically examined two complementary aspects of brain

alterations: the functional integrity of frontal networks (captured by pheno16) and structural damage associated with cerebral small vessel disease (indicated by WMH). Both traits represent biologically credible intermediates. Nonetheless, the Mendelian randomization results revealed no evidence that either functional network disruption (pheno16) or structural lesions (WMH) mediate the relationship between PhenoAge and ICH. This consistent pattern of null findings is itself highly informative, implying that PhenoAge may influence ICH risk through more proximal mechanisms that precede or bypass macroscopic brain changes detectable with fMRI or conventional MRI [49, 61-63]. Instead, PhenoAge may directly heighten the likelihood of vascular rupture by impairing microvascular integrity through processes such as endothelial dysfunction, compromised blood-brain barrier permeability, inflammation, or oxidative stress. This inference shifts the emphasis of future investigations from large-scale imaging phenotypes toward fundamental vascular biology, marking an important conceptual advance arising from the present study [63, 64].

The main strength of this study lies in its use of an MR design, which effectively overcomes the limitations of traditional observational studies and provides stronger evidence for causal inference [65, 66]. Multiple epigenetic markers and an innovative three-step mediation analysis approach were systematically evaluated. Furthermore, comprehensive sensitivity analyses ensured the robustness of our main conclusions.

However, this study also has some limitations. First, a major limitation of this study is that all GWAS summary statistics analyzed were derived exclusively from individuals of European ancestry. Given potential differences in genetic architecture, linkage disequilibrium patterns, and environmental exposures across ethnic groups, allele frequencies and the effect sizes of gene-outcome associations may vary accordingly. Consequently, the generalizability of our findings is restricted, and the conclusions

regarding the causal relationship between PhenoAge and ICH may not be directly generalizable to Asian, African, or other non-European populations. This is an important caveat that should be considered when interpreting our results. Confirming the robustness of these associations in multi-ethnic cohorts represents an important direction for future research. Nonetheless, the current unavailability of sufficiently large GWAS datasets for epigenetic aging and ICH in non-European populations constrained the scope of this analysis. Secondly, although our investigation incorporated both a functional connectivity marker (pheno16) and a critical structural indicator (WMH), we recognize that these two phenotypes do not fully capture the entire spectrum of brain alterations potentially implicated in ICH. Therefore, the absence of evidence for mediation in our study should not be interpreted as definitive evidence against neural mediation more broadly. Other relevant brain imaging metrics, including cerebral microbleeds or reductions in gray matter volume, remain unmeasured in our study and could plausibly serve as mediating factors. Comprehensive future studies employing a broader, multimodal neuroimaging strategy are essential to systematically delineate the neural substrates that bridge systemic aging processes with cerebrovascular outcomes. Third, the brain imaging phenotypes were based on resting-state fMRI functional connectivity nodes, whose biological interpretation is still evolving, and they do not fully represent all structural and functional changes in the brain. Additionally, our mediation analysis focused exclusively on a single brain imaging phenotype, pheno16. The limited statistical power of our mediation analysis necessitates a cautious interpretation of the null result regarding pheno16. Rather than constituting definitive evidence against mediation, this negative finding should be viewed as inconclusive, reflecting an inability to confirm a mediating role for pheno16 under current analytic constraints.

Moreover, we cannot exclude the possibility that mediation may occur through alternative, unexamined brain networks or via subtler pathways not captured by the present analysis. Finally, we applied multiple complementary sensitivity analyses (including MR-Egger and MR-PRESSO) to identify and adjust for horizontal pleiotropy; the potential for residual, unmeasured pleiotropy remains an intrinsic limitation of Mendelian randomization studies and cannot be fully excluded. This concern is particularly pertinent for the PhenoAge-pheno16 association, which became evident only after outlier removal. The SNPs excluded might influence brain function through biological mechanisms unrelated to epigenetic aging, introducing possible confounding and biasing our causal inference. Therefore, this finding should be interpreted with specific caution.

Conclusion

In conclusion, this study provides strong genetic evidence that accelerated biological aging, as measured by PhenoAge, is a causal risk factor for ICH. It also suggests that this systemic aging process may influence frontal lobe network function, although this pathway does not mediate the increased risk of ICH. These findings advance our etiological understanding by highlighting systemic biological aging as a key upstream driver of ICH, distinct from specific brain network changes.

Beyond its mechanistic insights, this work carries direct implications for prevention and prediction. By establishing PhenoAge acceleration as a causal, rather than merely correlative, risk factor, it provides a rationale for targeting the biological aging process itself in ICH prevention strategies. In clinical practice, PhenoAge could serve as a biomarker complementary to chronological age, helping to identify high-risk individuals for earlier and more intensive management of modifiable factors such as

hypertension. Ultimately, this research shifts the focus from managing downstream events to addressing upstream systemic decline, opening new avenues for risk stratification and preventive medicine in cerebrovascular disease. Future studies should further elucidate the molecular and vascular mechanisms linking epigenetic aging to cerebrovascular rupture.

Ethics approval and consent to participate

Not applicable.

Consent for publication

Not applicable.

Availability of data and materials

All data generated or analyzed during this study are included in this published article and its supplementary information files.

Competing interests

The authors declare that they have no competing interests.

Funding

This work was supported by the Guangzhou Science and Technology Project (Project Number 2023A04J2425).

Authors' contributions

Conception and design: Jianwei Guan

Administrative support: Qiang Wang

Provision of study materials or patients: Xinyu Cheng

Collection and assembly of data: Yunyao Li

Data analysis and interpretation: Yunyao Li

Manuscript writing: Yunyao Li, Xinyu Cheng, Qiang Wang, Jianwei Guan

Final approval of manuscript: Yunyao Li, Xinyu Cheng, Qiang Wang, Jianwei Guan

Acknowledgments

None.

REFERENCES

1. Faghih-Jouybari M, Raof MT, Abdollahzade S, et al. Mortality and morbidity in patients with spontaneous intracerebral hemorrhage: A single-center experience. Curr J Neurol 2021;20:32-36.

2. Rajashekar D, Liang JW. Intracerebral Hemorrhage. StatPearls. Treasure Island (FL)2025.

3. Stanton R, Demel SL, Flaherty ML, et al. Risk of intracerebral haemorrhage from hypertension is greatest at an early age. Eur Stroke J 2021;6:28-35.

4. Fransquet PD, Wrigglesworth J, Woods RL, Ernst ME, Ryan J. The epigenetic clock as a predictor of disease and mortality risk: a systematic review and meta-analysis. Clin Epigenetics 2019;11:62.

5. Morales Berstein F, McCartney DL, Lu AT, et al. Assessing the causal role of epigenetic clocks in the development of multiple cancers: a Mendelian randomization study. Elife 2022;11.

6. Guo Y, Zhang Y, Hu Y. COVID-19 subgroups may slow down biological age acceleration. J Infect 2023;86:66-117.

7. Fuentealba M, Rouch L, Guyonnet S, et al. A blood-based epigenetic clock for intrinsic capacity predicts mortality and is associated with clinical, immunological and lifestyle factors. Nature Aging 2025;5:1207-1216.

8. Klopack ET, Carroll JE, Cole SW, Seeman TE, Crimmins EM. Lifetime exposure to smoking, epigenetic aging, and morbidity and mortality in older adults. Clin Epigenetics 2022;14:72.

9. Margiotti K, Monaco F, Fabiani M, Mesoraca A, Giorlandino C. Epigenetic Clocks: In Aging-Related and Complex Diseases. Cytogenetic and Genome Research 2023;163:247-256.
10. Qiu B, Wen S, Li Z, et al. Causal Associations of Epigenetic Age Acceleration With Stroke and Its Functional Outcome: A Two-Sample, Two-Step Mendelian Randomization Study. Brain Behav 2025;15:e70412.
11. Maimaiti A, Ma J, Hao C, et al. DNA methylation-estimated phenotypes, telomere length and risk of ischemic stroke: epigenetic age acceleration of screening and a Mendelian randomization study. Aging (Albany NY) 2024;16:11970-11993.
12. Graves AJ, Danoff JS, Kim M, et al. Accelerated epigenetic age is associated with whole-brain functional connectivity and impaired cognitive performance in older adults. Sci Rep 2024;14:9646.
13. Wheater ENW, Stoye DQ, Cox SR, et al. DNA methylation and brain structure and function across the life course: A systematic review. Neuroscience & Biobehavioral Reviews 2020;113:133-156.
14. Marsland AL, Kuan DC, Sheu LK, et al. Systemic inflammation and resting state connectivity of the default mode network. Brain Behav Immun 2017;62:162-170.
15. Kapoor A, Jang JY, Engstrom AC, et al. Elevated vascular endothelial growth factor a is associated with disruption of default network connectivity in older adults. Brain Imaging Behav 2025;19:379-383.
16. Wirth M, Gaubert M, Köbe T, et al. Vascular Health Is Associated With Functional Connectivity Decline in Higher-Order Networks of Older Adults. Frontiers

in Integrative Neuroscience 2022;Volume 16 - 2022.

17. Stoklosa I, Marwaha R, Stoklosa M, et al. Neuroimaging in post-traumatic stress disorder: a narrative review. Arch Med Sci 2025;21:32-41.

18. Azarias FR, Almeida G, de Melo LF, Rici REG, Maria DA. The Journey of the Default Mode Network: Development, Function, and Impact on Mental Health. Biology (Basel) 2025;14.

19. Ereira S, Waters S, Razi A, Marshall CR. Early detection of dementia with default-mode network effective connectivity. Nature Mental Health 2024;2:787-800.

20. Siddiqui FM, Bekker SV, Qureshi AI. Neuroimaging of hemorrhage and vascular defects. Neurotherapeutics 2011;8:28-38.

21. Yang D, Luo X, Sun S, et al. Abnormal dynamic functional connectivity in young nondisabling intracerebral hemorrhage patients. Ann Clin Transl Neurol 2024;11:1567-1578.

22. Burgess S, Butterworth A, Thompson SG. Mendelian randomization analysis with multiple genetic variants using summarized data. Genet Epidemiol 2013;37:658-665.

23. Davey Smith G, Ebrahim S. 'Mendelian randomization': can genetic epidemiology contribute to understanding environmental determinants of disease? International journal of epidemiology 2003;32:1-22.

24. Davey Smith G, Hemani G. Mendelian randomization: genetic anchors for causal inference in epidemiological studies. Hum Mol Genet 2014;23:R89-98.

25. Burgess S, Thompson SG, Collaboration CCG. Avoiding bias from weak instruments in Mendelian randomization studies. International Journal of

Epidemiology 2011;40:755-764.

26. Li CY, Xie WX, You HP, Hu HR, Chen ZY. A multi-stage genomic approach to uncover druggable gene targets and neural pathways in postpartum depression. Arch Med Sci 2025;21:2047-2057.

27. Roberts JD, Vittinghoff E, Lu AT, et al. Epigenetic Age and the Risk of Incident Atrial Fibrillation. Circulation 2021;144:1899-1911.

28. McCartney DL, Min JL, Richmond RC, et al. Genome-wide association studies identify 137 genetic loci for DNA methylation biomarkers of aging. Genome Biol 2021;22:194.

29. Wang L, Xu S, Chen R, et al. Exploring the causal association between epigenetic clocks and menopause age: insights from a bidirectional Mendelian randomization study. Front Endocrinol (Lausanne) 2024;15:1429514.

30. Li Y, Chen J, Sun T, et al. Genetically determined telomere length and risk for haematologic diseases: results from large prospective cohorts and Mendelian Randomization analysis. Blood Cancer J 2024;14:48.

31. Kim JS, Azarbarzin A, Podolanczuk AJ, et al. Obstructive Sleep Apnea and Longitudinal Changes in Interstitial Lung Imaging and Lung Function: The MESA Study. Ann Am Thorac Soc 2023;20:728-737.

32. Tan H, Wang S, Huang F, Tong Z. Association between breast cancer and thyroid cancer risk: a two-sample Mendelian randomization study. Front Endocrinol (Lausanne) 2023;14:1138149.

33. Zhao Z, Cao Q, Zhu M, Wang C, Lu X. Causal relationships between serum

matrix metalloproteinases and estrogen receptor-negative breast cancer: a bidirectional mendelian randomization study. Sci Rep 2023;13:7849.

34. Lin Z, Deng Y, Pan W. Combining the strengths of inverse-variance weighting and Egger regression in Mendelian randomization using a mixture of regressions model. PLoS genetics 2021;17:e1009922.

35. Bowden J, Del Greco MF, Minelli C, Davey Smith G, Sheehan NA, Thompson JR. Assessing the suitability of summary data for two-sample Mendelian randomization analyses using MR-Egger regression: the role of the I2 statistic. Int J Epidemiol 2016;45:1961-1974.

36. Brion M-JA, Shakhbazov K, Visscher PM. Calculating statistical power in Mendelian randomization studies. International journal of epidemiology 2013;42:1497-1501.

37. Tabangin ME, Woo JG, Liu C, Nick TG, Martin LJ. Comparison of false-discovery rate for genome-wide and fine mapping regions. BMC Proc 2007;1 Suppl 1:S148.

38. Pereira TV, Patsopoulos NA, Salanti G, Ioannidis JP. Critical interpretation of Cochran's Q test depends on power and prior assumptions about heterogeneity. Research Synthesis Methods 2010;1:149-161.

39. Verbanck M, Chen CY, Neale B, Do R. Detection of widespread horizontal pleiotropy in causal relationships inferred from Mendelian randomization between complex traits and diseases. Nat Genet 2018;50:693-698.

40. Xu J, Ma J, Chen J, et al. No genetic causal association between iron status and

osteoporosis: A two-sample Mendelian randomization. Front Endocrinol (Lausanne) 2022;13:996244.

41. Bowden J, Spiller W, Del Greco MF, et al. Improving the visualization, interpretation and analysis of two-sample summary data Mendelian randomization via the Radial plot and Radial regression. Int J Epidemiol 2018;47:1264-1278.

42. Levine ME, Lu AT, Quach A, et al. An epigenetic biomarker of aging for lifespan and healthspan. Aging (Albany NY) 2018;10:573-591.

43. Ma Q, Li BL, Yang L, et al. Association between Phenotypic Age and Mortality in Patients with Multivessel Coronary Artery Disease. Dis Markers 2022;2022:4524032.

44. Bortz J, Guariglia A, Klaric L, et al. Biological age estimation using circulating blood biomarkers. Communications Biology 2023;6:1089.

45. Gao Y, Gao K, Shi R, et al. Association between phenotypic age and in-hospital outcomes in patients with acute myocardial infarction: A retrospective observational study. Int J Cardiol Heart Vasc 2025;58:101670.

46. Tjili TM, July J, Darwin E, et al. Vascular endothelial cadherin dysfunction: A predictor of hypertensive nonlobar intracerebral hemorrhage. Surg Neurol Int 2025;16:268.

47. Huang B, Chen A, Sun Y, He Q. The Role of Aging in Intracerebral Hemorrhage. Brain Sci 2024;14.

48. Zhang X, Zhao H, Li Z, et al. Accelerated biological aging, healthy behaviors, and genetic susceptibility with incidence of stroke and its subtypes: A prospective

cohort study. Aging Cell 2025;24:e14427.

49. Sant'Anna Barbosa Ferreira P, van Dongen J, den Braber A, Boomsma DI, de Geus EJC, van 't Ent D. Epigenetic age acceleration in peripheral blood correlates with brain-MRI age acceleration. Brain 2025;148:2861-2868.

50. Walton E, Baltramonaityte V, Calhoun V, Heijmans BT, Thompson PM, Cecil CAM. A systematic review of neuroimaging epigenetic research: calling for an increased focus on development. Molecular Psychiatry 2023;28:2839-2847.

51. Chand GB, Wu J, Hajjar I, Qiu D. Interactions of the Salience Network and Its Subsystems with the Default-Mode and the Central-Executive Networks in Normal Aging and Mild Cognitive Impairment. Brain Connect 2017;7:401-412.

52. Wei X, Qin W. Exploring causal links between brain functional networks and neurodegenerative disease risk using Mendelian randomization. J Alzheimers Dis Rep 2025;9:25424823251348844.

53. Schimmelpfennig J, Topczewski J, Zajkowski W, Jankowiak-Siuda K. The role of the salience network in cognitive and affective deficits. Front Hum Neurosci 2023;17:1133367.

54. Zhang HY, Chen WX, Jiao Y, Xu Y, Zhang XR, Wu JT. Selective vulnerability related to aging in large-scale resting brain networks. PLoS One 2014;9:e108807.

55. Filippi M, Cividini C, Basaia S, et al. Age-related vulnerability of the human brain connectome. Molecular Psychiatry 2023;28:5350-5358.

56. Knox EG, Aburto MR, Clarke G, Cryan JF, O'Driscoll CM. The blood-brain barrier in aging and neurodegeneration. Mol Psychiatry 2022;27:2659-2673.

57. Elliott ML, Belsky DW, Knodt AR, et al. Brain-age in midlife is associated with accelerated biological aging and cognitive decline in a longitudinal birth cohort. Mol Psychiatry 2021;26:3829-3838.

58. Wardlaw JM, Smith C, Dichgans M. Mechanisms of sporadic cerebral small vessel disease: insights from neuroimaging. Lancet Neurol 2013;12:483-497.

59. van den Heuvel MP, Sporns O. A cross-disorder connectome landscape of brain dysconnectivity. Nat Rev Neurosci 2019;20:435-446.

60. Zalesky A, Fornito A, Bullmore ET. Network-based statistic: identifying differences in brain networks. Neuroimage 2010;53:1197-1207.

61. Markus HS, de Leeuw FE. Cerebral small vessel disease: Recent advances and future directions. International Journal of Stroke 2022;18:4-14.

62. Bhagat R, Marini S, Romero JR. Genetic considerations in cerebral small vessel diseases. Frontiers in Neurology 2023;Volume 14 - 2023.

63. Huang H, Song W, Wang P, et al. White Matter Hyperintensities: Cerebral Small-Vessel Diseases and White Matter Microstructural Impairments. iRADIOLOGY 2025;3:5-25.

64. Ungvari Z, Tarantini S, Donato AJ, Galvan V, Csiszar A. Mechanisms of Vascular Aging. Circ Res 2018;123:849-867.

65. Richmond RC, Davey Smith G. Mendelian Randomization: Concepts and Scope. Cold Spring Harb Perspect Med 2022;12.

66. Sanderson E, Glymour MM, Holmes MV, et al. Mendelian randomization. Nat Rev Methods Primers 2022;2.

FIGURE LEGENDS

Figure 1. The flow diagram of the process in this Mendelian randomization analysis

Figure 2. The association between PhenoAge and the risk of ICH is presented in (A) a forest plot, (B) a leave-one-out sensitivity analysis, (C) a scatter plot, and (D) a funnel plot, as part of a forward analysis.

Table 1. Genetics predicts associations between epigenetic clocks and ICH (no outlier removal)

Outcome	Exposure	N.SNP	Methods	OR (CI)	P-value	FDR
ICH	PhenoAge	11	Inverse variance weighted	1.07932 (1.0333-1.1273)	6e-04	0.0035
ICH	PhenoAge	11	MR Egger	1.20894 (1.0583-1.381)	0.0209	0.1253
ICH	PhenoAge	11	Weighted median	1.09097 (1.0271-1.1588)	0.0047	0.0279
ICH	PhenoAge	11	Weighted mode	1.11490 (1.0105-1.2301)	0.0553	0.3316
ICH	PAI1	5	Inverse variance weighted	0.99993 (0.9998-1)	0.2242	0.416
ICH	PAI1	5	MR Egger	1.00007 (0.9998-1.0003)	0.6136	0.6136
ICH	PAI1	5	Weighted median	0.99991 (0.9998-1)	0.1783	0.3566
ICH	PAI1	5	Weighted mode	0.99990 (0.9998-1)	0.2644	0.5289
ICH	HorvathAge	24	Inverse variance weighted	0.99710 (0.9577-1.0381)	0.8877	0.8877
ICH	HorvathAge	24	MR Egger	1.03384 (0.9396-1.1376)	0.5022	0.6027
ICH	HorvathAge	24	Weighted median	1.00868 (0.9542-1.0663)	0.7603	0.9123
ICH	HorvathAge	24	Weighted mode	1.01374 (0.9386-1.0949)	0.7314	0.7448

ICH	HannumAge	9	Inverse variance weighted	0.97403 (0.9112-1.0411)	0.4389	0.5267
ICH	HannumAge	9	MR Egger	0.84595 (0.6571-1.0891)	0.2354	0.4709
ICH	HannumAge	9	Weighted median	0.97358 (0.8895-1.0656)	0.5611	0.8416
ICH	HannumAge	9	Weighted mode	0.98102 (0.8775-1.0967)	0.7448	0.7448
ICH	GrimAge	27	Inverse variance weighted	0.96649 (0.9197-1.0156)	0.1778	0.416
ICH	GrimAge	27	MR Egger	0.94895 (0.8527-1.056)	0.3459	0.5189
ICH	GrimAge	27	Weighted median	0.95008 (0.8898-1.0144)	0.1257	0.3566
ICH	GrimAge	27	Weighted mode	0.93749 (0.8518-1.0318)	0.1982	0.5289
ICH	granulocyte proportions	17	Inverse variance weighted	0.24818 (0.0201-3.0675)	0.2773	0.416
ICH	granulocyte proportions	17	MR Egger	0.00574 (0-6.072)	0.167	0.4709
ICH	granulocyte proportions	17	Weighted median	0.89585 (0.0281-28.5738)	0.9504	0.9504
ICH	granulocyte proportions	17	Weighted mode	3.22353 (0.0072-1437.3218)	0.7118	0.7448

Table 2. Genetics predicts associations between epigenetic clocks and brain imaging phenotypes (before outlier removal)

outcome	exposure	N.SNP	Methods	OR_CI	P-value	FDR
pheno9	PhenoAge	11	Inverse variance weighted	1.007 (0.988-1.03)	0.4803	0.8769
pheno9	PhenoAge	11	MR Egger	1.039 (0.984-1.10)	0.1991	0.9571
pheno9	PhenoAge	11	Weighted median	1.016 (0.994-1.04)	0.1558	0.4037
pheno9	PhenoAge	11	Weighted mode	1.018 (0.991-1.05)	0.2258	0.6783
pheno8	PhenoAge	11	Inverse variance weighted	1.012 (0.996-1.03)	0.145	0.7932
pheno8	PhenoAge	11	MR Egger	1.011 (0.966-1.06)	0.6579	0.9571
pheno8	PhenoAge	11	Weighted median	1.013 (0.993-1.03)	0.1998	0.4037
pheno8	PhenoAge	11	Weighted mode	1.012 (0.985-1.04)	0.407	0.6783
pheno7	PhenoAge	11	Inverse variance weighted	1.001 (0.982-1.02)	0.9391	0.9762
pheno7	PhenoAge	11	MR Egger	0.989 (0.934-1.05)	0.6999	0.9571
pheno7	PhenoAge	11	Weighted median	1.002 (0.980-1.03)	0.8528	0.9005
pheno7	PhenoAge	11	Weighted mode	0.999 (0.967-1.03)	0.9382	0.9405

pheno5	PhenoAge	11	Inverse variance weighted	1.005 (0.982-1.03)	0.6983	0.969
pheno5	PhenoAge	11	MR Egger	1.012 (0.945-1.08)	0.7437	0.9571
pheno5	PhenoAge	11	Weighted median	1.007 (0.984-1.03)	0.5741	0.6754
pheno5	PhenoAge	11	Weighted mode	1.004 (0.976-1.03)	0.7815	0.9405
pheno4	PhenoAge	11	Inverse variance weighted	1.012 (0.996-1.03)	0.1309	0.7932
pheno4	PhenoAge	11	MR Egger	1.022 (0.976-1.07)	0.3793	0.9571
pheno4	PhenoAge	11	Weighted median	1.014 (0.993-1.04)	0.1845	0.4037
pheno4	PhenoAge	11	Weighted mode	1.014 (0.986-1.04)	0.3539	0.6783
pheno3	PhenoAge	11	Inverse variance weighted	1.000 (0.978-1.02)	0.9762	0.9762
pheno3	PhenoAge	11	MR Egger	1.014 (0.949-1.08)	0.6841	0.9571
pheno3	PhenoAge	11	Weighted median	1.008 (0.984-1.03)	0.5219	0.6524
pheno3	PhenoAge	11	Weighted mode	1.010 (0.977-1.04)	0.5696	0.8137
pheno21	PhenoAge	11	Inverse variance weighted	1.010 (0.989-1.03)	0.3638	0.8083
pheno21	PhenoAge	11	MR Egger	1.025 (0.961-1.09)	0.4737	0.9571
pheno21	PhenoAge	11	Weighted median	1.019 (0.997-1.04)	0.0899	0.3598

pheno21	PhenoAge	11	Weighted mode	1.019 (0.992-1.05)	0.1912	0.6783
pheno20	PhenoAge	11	Inverse variance weighted	1.004 (0.984-1.02)	0.6912	0.969
pheno20	PhenoAge	11	MR Egger	1.021 (0.964-1.08)	0.4934	0.9571
pheno20	PhenoAge	11	Weighted median	1.022 (1.000-1.04)	0.0483	0.3552
pheno20	PhenoAge	11	Weighted mode	1.025 (0.994-1.06)	0.1415	0.6783
pheno2	PhenoAge	11	Inverse variance weighted	1.010 (0.994-1.03)	0.2419	0.7932
pheno2	PhenoAge	11	MR Egger	1.047 (1.000-1.10)	0.0814	0.9571
pheno2	PhenoAge	11	Weighted median	1.014 (0.992-1.04)	0.2154	0.4037
pheno2	PhenoAge	11	Weighted mode	1.015 (0.982-1.05)	0.3929	0.6783
pheno19	PhenoAge	11	Inverse variance weighted	1.013 (0.998-1.03)	0.0943	0.7932
pheno19	PhenoAge	11	MR Egger	1.029 (0.984-1.08)	0.2469	0.9571
pheno19	PhenoAge	11	Weighted median	1.020 (0.998-1.04)	0.071	0.3552
pheno19	PhenoAge	11	Weighted mode	1.020 (0.990-1.05)	0.2159	0.6783
pheno18	PhenoAge	11	Inverse variance weighted	1.012 (0.993-1.03)	0.2186	0.7932
pheno18	PhenoAge	11	MR Egger	1.003 (0.947-1.06)	0.9154	0.9571

pheno18	PhenoAge	11	Weighted median	1.009 (0.987-1.03)	0.4365	0.6259
pheno18	PhenoAge	11	Weighted mode	1.001 (0.968-1.04)	0.9405	0.9405
pheno17	PhenoAge	11	Inverse variance weighted	1.007 (0.987-1.03)	0.4823	0.8769
pheno17	PhenoAge	11	MR Egger	1.007 (0.947-1.07)	0.8366	0.9571
pheno17	PhenoAge	11	Weighted median	1.008 (0.987-1.03)	0.4381	0.6259
pheno17	PhenoAge	11	Weighted mode	1.004 (0.975-1.03)	0.7949	0.9405
pheno16	PhenoAge	11	Inverse variance weighted	1.013 (0.986-1.04)	0.3467	0.8083
pheno16	PhenoAge	11	MR Egger	1.012 (0.935-1.10)	0.767	0.9571
pheno16	PhenoAge	11	Weighted median	1.017 (0.994-1.04)	0.1551	0.4037
pheno16	PhenoAge	11	Weighted mode	1.015 (0.986-1.05)	0.3401	0.6783
pheno15	PhenoAge	11	Inverse variance weighted	1.009 (0.993-1.03)	0.2776	0.7932
pheno15	PhenoAge	11	MR Egger	1.027 (0.982-1.08)	0.2729	0.9571
pheno15	PhenoAge	11	Weighted median	1.009 (0.988-1.03)	0.4112	0.6259
pheno15	PhenoAge	11	Weighted mode	1.013 (0.985-1.04)	0.39	0.6783
pheno14	PhenoAge	11	Inverse variance weighted	1.007 (0.983-1.03)	0.5761	0.9601

pheno14	PhenoAge	11	MR Egger	1.008 (0.938-1.08)	0.8407	0.9571
pheno14	PhenoAge	11	Weighted median	1.026 (1.002-1.05)	0.0361	0.3552
pheno14	PhenoAge	11	Weighted mode	1.033 (0.993-1.07)	0.1358	0.6783
pheno13	PhenoAge	11	Inverse variance weighted	1.015 (0.992-1.04)	0.2136	0.7932
pheno13	PhenoAge	11	MR Egger	1.023 (0.956-1.10)	0.5234	0.9571
pheno13	PhenoAge	11	Weighted median	1.021 (0.998-1.04)	0.0687	0.3552
pheno13	PhenoAge	11	Weighted mode	1.020 (0.992-1.05)	0.1891	0.6783
pheno12	PhenoAge	11	Inverse variance weighted	1.002 (0.983-1.02)	0.8761	0.9735
pheno12	PhenoAge	11	MR Egger	0.984 (0.931-1.04)	0.5763	0.9571
pheno12	PhenoAge	11	Weighted median	1.000 (0.979-1.02)	0.9883	0.9883
pheno12	PhenoAge	11	Weighted mode	1.003 (0.975-1.03)	0.8581	0.9405
pheno11	PhenoAge	11	Inverse variance weighted	0.996 (0.976-1.02)	0.7431	0.969
pheno11	PhenoAge	11	MR Egger	0.998 (0.937-1.06)	0.9571	0.9571
pheno11	PhenoAge	11	Weighted median	0.986 (0.965-1.01)	0.222	0.4037
pheno11	PhenoAge	11	Weighted mode	0.981 (0.950-1.01)	0.2651	0.6783

pheno10	PhenoAge	11	Inverse variance weighted	1.003 (0.983-1.02)	0.7752	0.969
pheno10	PhenoAge	11	MR Egger	1.003 (0.946-1.06)	0.9107	0.9571
pheno10	PhenoAge	11	Weighted median	1.002 (0.980-1.03)	0.8555	0.9005
pheno10	PhenoAge	11	Weighted mode	1.003 (0.972-1.04)	0.8407	0.9405
pheno1	PhenoAge	11	Inverse variance weighted	0.998 (0.973-1.02)	0.8619	0.9735
pheno1	PhenoAge	11	MR Egger	1.027 (0.955-1.10)	0.4935	0.9571
pheno1	PhenoAge	11	Weighted median	1.008 (0.986-1.03)	0.4824	0.6432
pheno1	PhenoAge	11	Weighted mode	1.010 (0.983-1.04)	0.4955	0.7624

Table 3. Genetics predicts associations between brain imaging phenotypes and ICH (before outlier removal)

outcome	exposure	N.SNP	Methods	OR_CI	P-value	FDR
ICH	pheno16	17	Inverse variance weighted	0.913 (0.712-1.171)	0.4753	0.4753
ICH	pheno16	17	MR Egger	0.405 (0.192-0.855)	0.0315	0.0315
ICH	pheno16	17	Weighted median	0.863 (0.694-1.074)	0.1869	0.1869
ICH	pheno16	17	Weighted mode	0.883 (0.683-1.143)	0.3601	0.3601

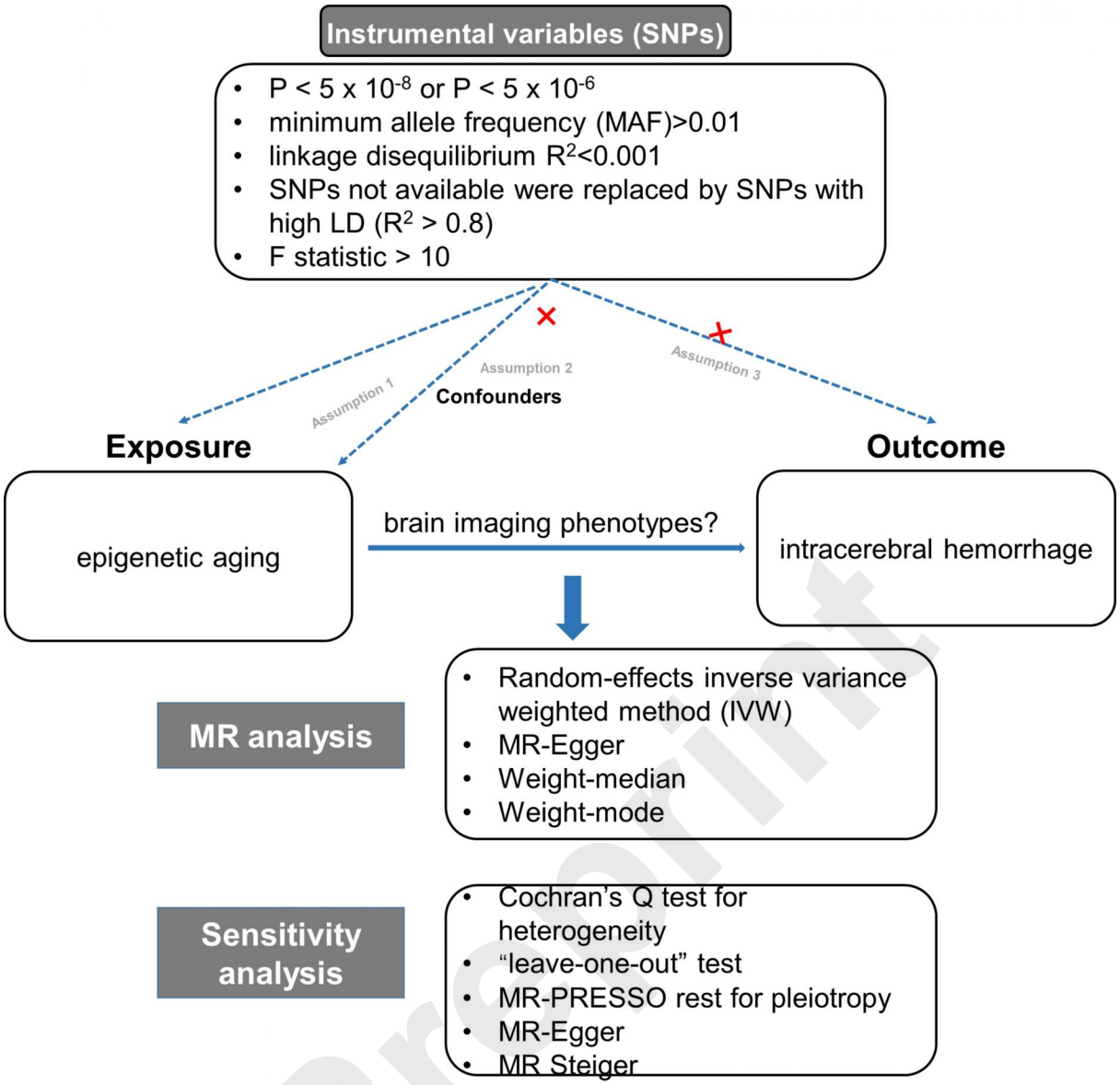
Instrumental variables (SNPs)
P < 5 x 10-8 or P < 5 x 10-6
minimum allele frequency (MAF)>0.01
linkage disequilibrium R2<0.001
SNPs not available were replaced by SNPs with high LD (R2 > 0.8)
F statistic > 10
Assumption 1
Assumption 2
Assumption 3
Confounders
Exposure
Outcome
epigenetic aging
brain imaging phenotypes?
intracerebral hemorrhage
MR analysis
Random-effects inverse variance weighted method (IVW)
MR-Egger
Weight-median
Weight-mode
Sensitivity analysis
Cochran's Q test for heterogeneity
"leave-one-out" test
MR-PRESSO rest for pleiotropy
MR-Egger
MR Steiger

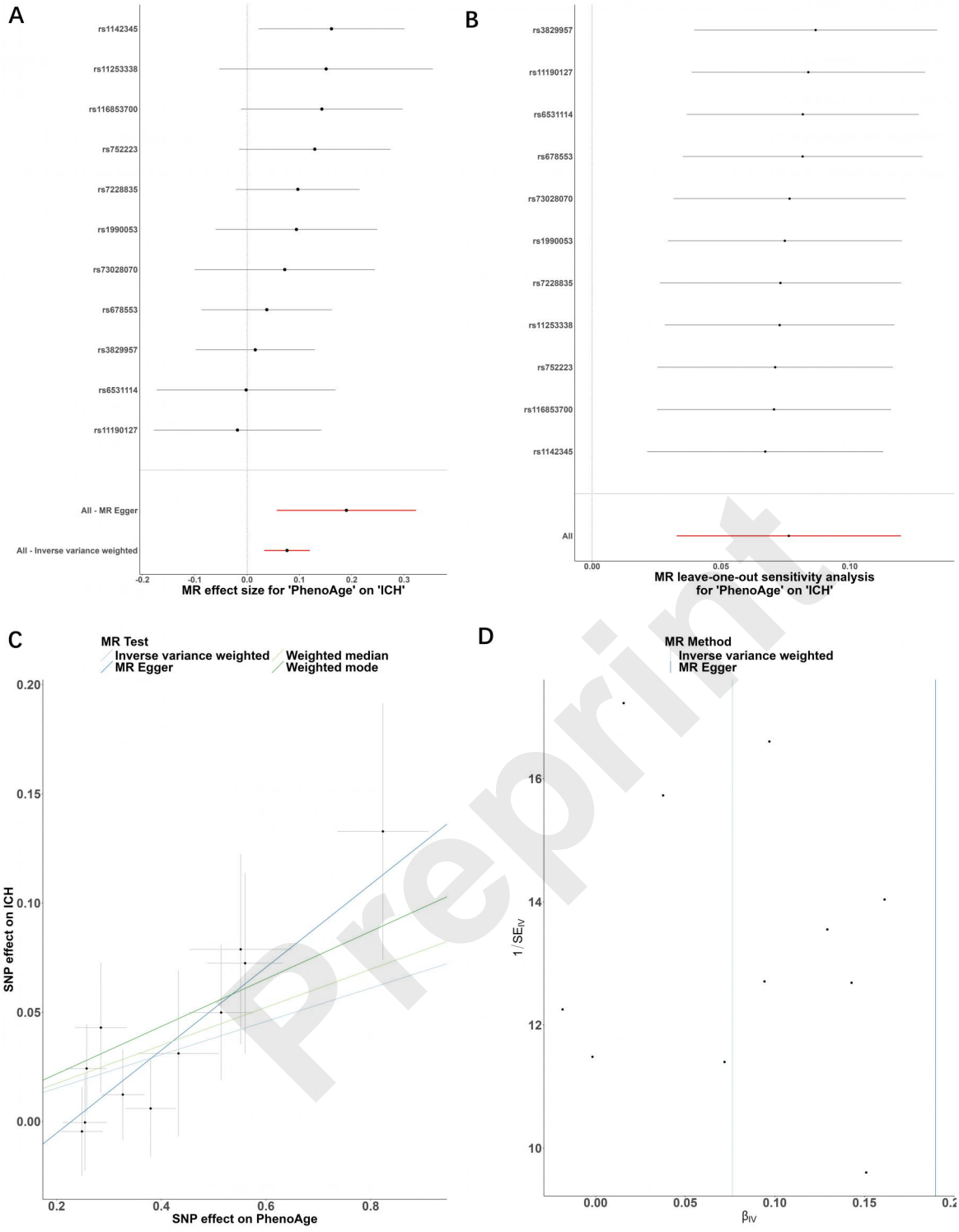
A
rs1142345
rs11253338
rs116853700
rs752223
rs7228835
rs1990053
rs73028070
rs678553
rs3829957
rs6531114
rs11190127
All - MR Egger
All - Inverse variance weighted
-0.2
-0.1
0.0
0.1
0.2
0.3
MR effect size for 'PhenoAge' on 'ICH'
B
rs3829957
rs11190127
rs6531114
rs678553
rs73028070
rs1990053
rs7228835
rs11253338
rs752223
rs116853700
rs1142345
All
0.00
0.05
0.10
MR leave-one-out sensitivity analysis
for 'PhenoAge' on 'ICH'
C
MR Test
Inverse variance weighted
MR Egger
Weighted median
Weighted mode
0.20
0.15
0.10
0.05
0.00
SNP effect on ICH
0.2
0.4
0.6
0.8
SNP effect on PhenoAge
D
MR Method
Inverse variance weighted
MR Egger
16
14
12
10
1 / SE_IV
0.00
0.05
0.10
0.15
β_IV

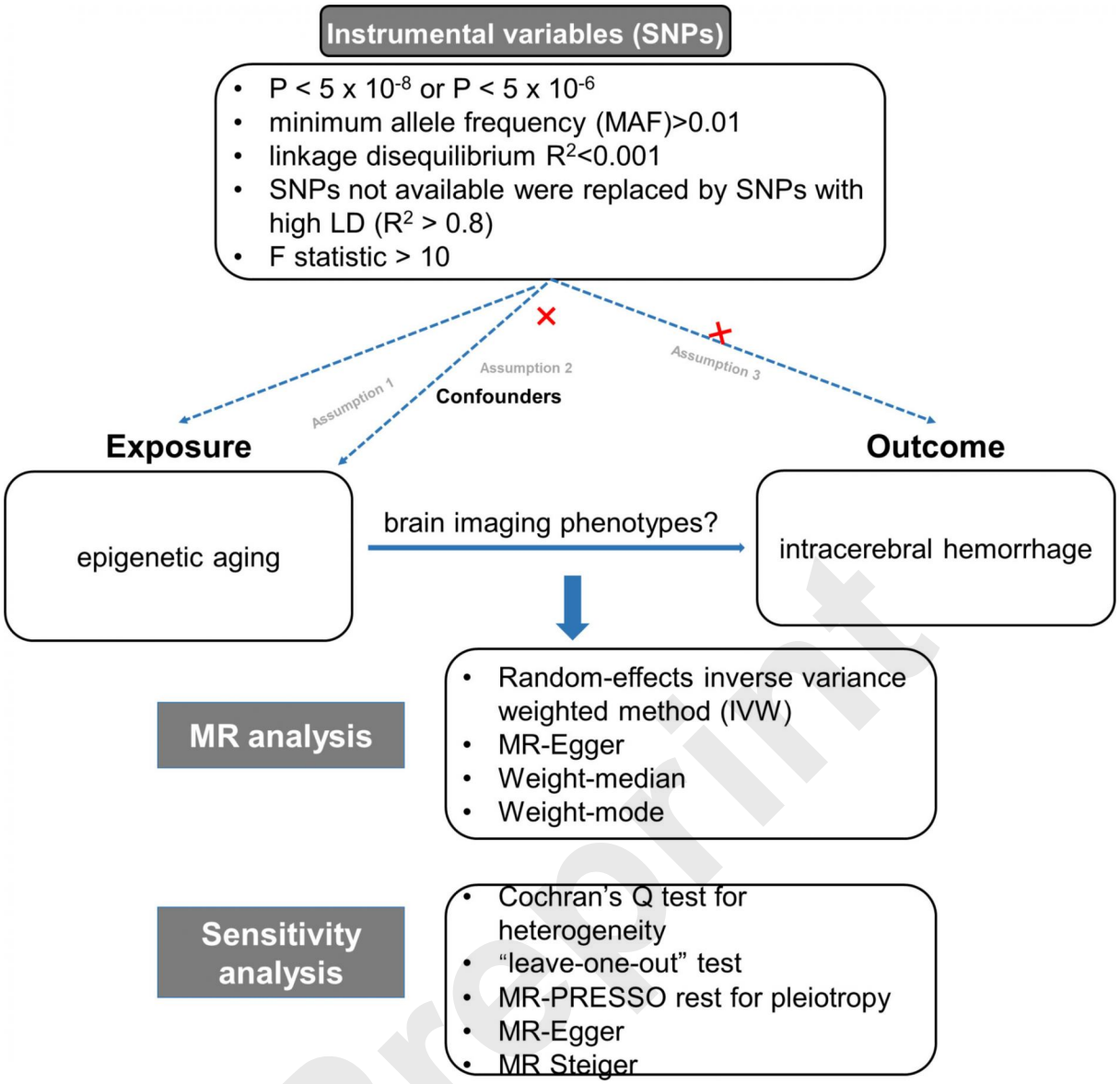
Instrumental variables (SNPs)
P < 5 x 10-8 or P < 5 x 10-6
minimum allele frequency (MAF)>0.01
linkage disequilibrium R2<0.001
SNPs not available were replaced by SNPs with high LD (R2 > 0.8)
F statistic > 10
Assumption 1
Assumption 2
Assumption 3
Confounders
Exposure
Outcome
epigenetic aging
brain imaging phenotypes?
intracerebral hemorrhage
MR analysis
Random-effects inverse variance weighted method (IVW)
MR-Egger
Weight-median
Weight-mode
Sensitivity analysis
Cochran's Q test for heterogeneity
"leave-one-out" test
MR-PRESSO rest for pleiotropy
MR-Egger
MR Steiger